Neural Computing and Applications
https://doi.org/10.1007/s00521-024-10219-w

ORIGINAL ARTICLE

A lightweight deep learning architecture for malaria parasite-type classification and life cycle stage detection

Hafiza Ayesha Hoor Chaudhry[1] · Muhammad Shahid Farid[2] · Attilio Fiandrotti[1] · Marco Grangetto[1]

Received: 14 December 2023 / Accepted: 12 July 2024

Abstract
Malaria is an endemic in various tropical countries. The gold standard for disease detection is to examine the blood smears of patients by an expert medical professional to detect malaria parasite called *Plasmodium*. In the rural areas of underdeveloped countries, with limited infrastructure, a scarcity of healthcare professionals, an absence of sufficient computing devices, and a lack of widespread internet access, this task becomes more challenging. A severe case of malaria can be fatal within one week, so the correct detection of the malaria parasite and its life cycle stage is crucial in treating the disease correctly. Though computer vision-based malaria detection has been adequately explored lately, the malaria life cycle stage classification is still a relatively unexplored field. In this paper, we introduce a fast and robust deep learning methodology to not only classify the malaria parasite-type detection but also the life cycle stage identification of the infected cell. The proposed deep learning architecture is more than twenty times lighter than the widely used DenseNet and has less than 0.4 million parameters, making it a good candidate to be used in the mobile applications of such economically challenged states for malaria detection. We have used four different publicly available malaria datasets to test the proposed architecture and gained significantly better results than the current state of the art on malaria parasite-type and malaria life cycle classification.

Keywords Medical image classification · Deep learning · Malaria detection · Malaria life cycle stage classification

1 Introduction

Malaria is a fatal disease caused by the *Plasmodium* parasite. It is endemic in Pakistan, with 3.4 million suspected cases of malaria from January to August in year 2022. These numbers rose rapidly as compared with the 2.6 million cases reported in 2021, due to a surge of floods in the country, and are expected to rise again in 2023 [1]. Other regions with the highest outbreaks of malaria are sub-Saharan Africa, South-East Asia, Western Pacific, and Eastern Mediterranean [2]. Malaria has been labeled as the disease of poverty, resulting from lower socio-economic and hygiene circumstances [3].

The malaria parasite is introduced into the host's body by a carrier mosquito and uses the red blood cells (RBCs) to carry out its life cycle. There are four types of malaria parasite known as *Plasmodium (P.) falciparum*, *P. vivax*, *P. ovale*, and *P. malariae*; the first two are the most common [4]. These parasite types target RBCs of a specific age, i.e., *malariae* targets old RBCs, whereas *vivax* targets young RBCs [5]. These types also have different lifespans and maturing ages than each other; some types can lay dormant for weeks and even relapse after the first infection [6]. Hence, it is important to diagnose not only the infection but also the parasite type in infected cells. Each parasite type has four stages in its life cycle: gametocyte, ring, schizont, and trophozoite [7]. The correct diagnosis of

✉ Hafiza Ayesha Hoor Chaudhry
hafizaayeshahoor.chaudhry@unito.it

Muhammad Shahid Farid
shahid@pucit.edu.pk

Attilio Fiandrotti
attilio.fiandrotti@unito.it

Marco Grangetto
marco.grangetto@unito.it

[1] Department of Computer Science, University of Turin, Torino 10149, Italy

[2] Department of Computer Science, University of the Punjab, Lahore 54590, Pakistan

Published online: 08 August 2024

the parasite life cycle stage is crucial for the proper treatment of this disease as various life cycle stages need more imminent care. Ring and trophozoite are the early stages of the parasite where the patients are mostly asymptotic (showing no symptoms of disease); hence, catching the disease at this stage ensures organ safety and patient survival chances [8]. However, there is little work done in classifying all the life cycle stages of the different types of malaria parasites as compared to the identification and detection of malaria parasite.

The standard malaria diagnosis method includes manually examining the blood slides under a microscope; if the parasite is found within red blood cells, then further investigation is done to detect the type, life cycle stage, and the total number of infected RBCs [9]. The accuracy of this method is directly dependent on the pathologists' expertise and the available infrastructure. Examining hundreds of large samples can be time-consuming, and a shortage of skilled pathologists could result in a misdiagnosis, especially in the already overwhelmed medical centers in endemic flooded areas like Pakistan [10]. The test procedure is not only time-consuming but also expensive given the costs of man-hours being used for this task. Computer-aided diagnosis (CAD) systems can relieve this load to a great extent while ensuring a lesser error rate and faster results at a cheaper cost. Previously traditional image processing techniques have been used to detect the malaria parasite and its types depending upon the morphological features of cells and image intensity values [11, 12]. Now there are more robust machine learning and deep learning architectures like convolutional neural networks (CNNs) that provide better results and are more preferred [13]. However, these deep learning architectures also require good-quality network coverage and hardware to function accurately. In countries facing economic disparities, where rural and remote areas encounter challenges in accessing reliable computer hardware and good internet connectivity, CAD systems cannot be incorporated due to their high computation cost. Thus, there is a need for a deep learning methodology that works with minimal computational cost, is lightweight to be embedded in mobile devices, and requires no internet or additional digital tools.

In this paper, we use deep learning to classify the various malaria parasite types and life cycle stages using a lightweight model that can be easily integrated into mobile applications for broad and enhanced user accessibility in remote and financially challenged areas. The main contributions and advantages of this paper are:

- Introduction of a novel lightweight deep learning (DL) architecture to classify both malaria parasite type and life cycle stage.
- Unlike most existing proposals which use multiple DL architecture pipelines for malaria classification and stage detection, e.g., [14], the proposed model is a single, lightweight architecture.
- Ablation study and experiments conducted to show the proposed architecture give better results than the state of the art while being less computationally expensive.

2 Literature review

Several computer-aided diagnosis (CAD) systems have been developed for the classification of malaria parasites from the blood slide images [15–17]. These systems take blood slide images of patients as input and classify the blood cells as infected or not infected, also called the binary classification of malaria [18]. Most public malaria datasets also have only two labels, healthy and infected, along with the blood slide images [19, 20].

The conventional classification of malaria includes using the morphological features of blood cells to identify the infected cells [21], along with improving the image acquisition method [22], and incorporating the image intensity information with the size of cells [23]. Some studies have altered full image color spaces to find the number of healthy and infected red blood cells [24], whereas color-based pixel discrimination has also been used for malaria cell detection [25]. The research in [26] uses histogram equalization and connected components to estimate the malaria parasite density. These traditional image processing methods are time-consuming and dependent on the features that vary between different datasets, e.g., intensity, prominent image color due to the staining technique used, etc. To further improve the results and speed up the process, machine learning and deep learning architectures were introduced as a much faster and more efficient alternative for the purpose of image classification.

The machine learning techniques range from using stacked CNNs for binary classification of malaria [27] to more sophisticated deep learning architectures for better accuracy [28]. Pre-trained neural networks along with optimization techniques have been used to achieve a higher accuracy in binary classification of malaria [29, 30] and to automatically detect malaria parasite from the given blood slide images [19].

Moving toward the multiclass classification of malaria parasite types, a few datasets provide the multiclass labels for various types of malaria parasites [31] and the area is relatively less explored. Kassim et al. [32] have worked on classifying *P. Falciparum* and *P. Vivax* from thick smear images. Recently, new datasets have been published that

include not only the type of malaria parasite with blood slides images but also have the multiclass labels for the life cycle stage, e.g., [14]. Their proposed method segments and classifies the malaria life cycle stage using deep learning architectures of pre-trained neural networks. Loddo et al. [33] also worked on a subset of [31] for the multiclass classification of life cycle stage using only the blood slide images of P. Falciparum malaria type. Several pre-trained networks were used, and DenseNet outperformed all the other networks for this task. Another malaria life cycle classifier is presented in [34] which classifies the malaria parasite using the ring, schizont, and trophozoite stages. Recent studies have used AlexNet and GoogleNet for the life cycle classification of Plasmodium parasite using data collected from the Hospital Universiti Sains Malaysia (HUSM). The GoogleNet Network and AlexNet showed an accuracy of 91.1% and 89.1% on test data respectively [35]. Another study used deep neural networks for the classification of the Plasmodium parasite into four known life cycle stages (ring, schizont, trophozoite, and gametocyte) where the Efficient Net B7 achieved an accuracy of 87.95% outperforming the other networks [36].

Most of the reviewed studies in this literature use traditional image processing techniques that are dependent on the features of a specific dataset and hence can't be used on others. Some recent studies have, however, used deep learning models on a malaria dataset that is too small or on a subset of the existing malaria dataset, eliminating some classes of either the malaria parasite type or life cycle stage. Our study provides a comprehensive network that classifies all the common classes of malaria parasite type and life cycle stage classification. Moreover, the deep learning networks used in recent studies are computationally expensive to be embedded in the inferior quality hardware available in remote areas of lower economically developed countries. Furthermore, a huge literature gap exists due to the high imbalance between the amount of work done in binary classification versus the multiclass classification of malaria parasite type. This research not only fills this gap but also provides more insight into the life cycle stages of malaria-infected cells. This malaria life cycle stage detection is an important key in planning the correct treatment and dosage of medicine, and ultimately saving many lives. Besides, there is a need for a methodology that is robust and independent of the varying features between different datasets. We also cater to this issue by using various public datasets and validating our methodology on all those. The rest of the paper is organized as follows, the benchmark malaria datasets used for testing the proposed technique are introduced in Sect. 3. Section 4 introduces the proposed methodology for malaria detection and classification. The experimental evaluations and discussion are presented in Sect. 5, and conclusions are drawn in Sect. 6.

3 Datasets

In this section, we briefly introduce the benchmark malaria datasets MP-IDB, MP-IDB2, IML_Malaria, and Malaria-Detection-2019 that we used in our experiments and performance evaluations.

3.1 MP-IDB

The MP-IDB [31] is a publicly available[1] malaria dataset collected at Centre Hospitalier Universitaire Vaudois (CHUV) using an optical laboratory microscope coupled with a built-in camera. There are a total of 229 full-slide blood images of four types of malaria parasites, *P. falciparum*, *P. vivax*, *P. malariae*, and *P. ovale*. These full-slide images have a resolution of 2592×1944 and are stored in PNG format with 24-bit color depth. The sample images of MP-IDB full-slide blood images are presented in Fig. 1.

Each parasite type is further divided into four life cycle stages, called ring, schizont, trophozoite, and gametocyte. For the life cycle stages, cell crops of varying resolutions are provided in PNG format, this dataset is referred to as MP-IDB2. The same microscope is used for acquiring all the images but the images vary in terms of illumination, background uniformity, and image border overexposure. The sample images of cell crops are presented in Fig. 2.

3.2 IML_Malaria

The IML_Malaria [14] is a benchmark dataset for malaria life cycle classification in thin blood smear images containing Giesema-stained full blood slide images of the malaria parasite. The dataset was first published in 2021 and contains 345 microscopic images. The images have a resolution of 1280×960 and are provided in a JPG format. An annotation file is also given along with the dataset that contains JSON arrays for each image. There are two keys for each JSON object, named as 'image_name' and 'objects'. The objects array further has the 'type' of each cell visible on the image and its bounding box called 'bbox'. The types of blood cell range from 'red blood cell', 'ring', 'schizont', 'trophozoite', 'gametocyte', and 'difficult'. The dataset is publicly available.[2] Sample images of this dataset are shown in Fig. 3.

[1] https://github.com/andrealoddo/MP-IDB-The-Malaria-Parasite-Image-Database-for-Image-Processing-and-Analysis.

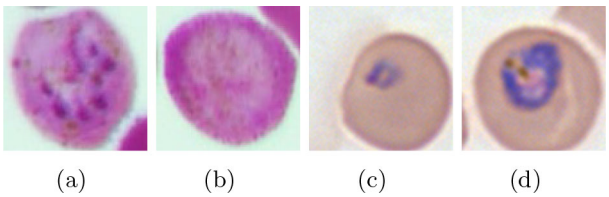

Fig. 1 Sample images from MP-IDB dataset: **a** *Falciparum*, **b** *Vivax*, **c** *Ovale*, and **d** *Malariae*

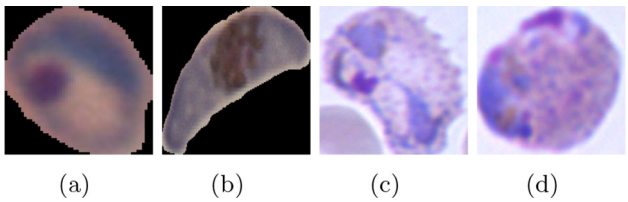

Fig. 2 Sample images from MP-IDB2 dataset: **a** Falciparum Ring, **b** Falciparum Gametocyte, **c** Vivax Schizont, and **d** Vivax Trophozoite

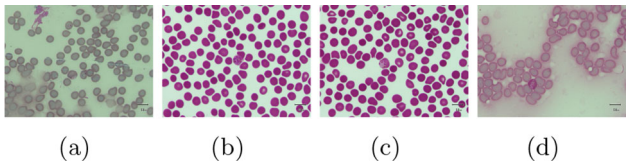

Fig. 3 Sample images from IML_Malaria dataset: **a** ring, **b** schizont, **c** trophozoite, and **d** *vivax* trophozoite

3.3 Malaria-Detection-2019

The Malaria-Detection-2019 dataset [34] is publicly available.[3] It contains 883 Giesema-stained full blood slide images from the malaria parasite. The images have a resolution of 1382 × 1030 in PNG format. The life cycle stage labels are provided along with the dataset. There are a total of eight labels for life cycle stages including early trophozoite (LR-ET), mid trophozoite (MT), ring (R), late ring, segmenter (Seg), early schizont (Esch), late schizont (Lsch), white blood cells (WBC), and debris. In their work [34], distinguishing between all eight stages was becoming very difficult, especially the early and late labels of each life cycle stage. Therefore, these eight stages were merged and finalized into three stages instead, ring, schizont, and trophozoite to increase the accuracy. We will also follow the same strategy in this research. A few images of these three stages are shown in Fig. 4.

[2] https://github.com/QaziAmmar/A-dataset-and-benchmark-for-malaria-life-cycle-classification-in-thin-blood-smear-images.

[3] https://data.mendeley.com/datasets/5bf2kmwvfn/1.

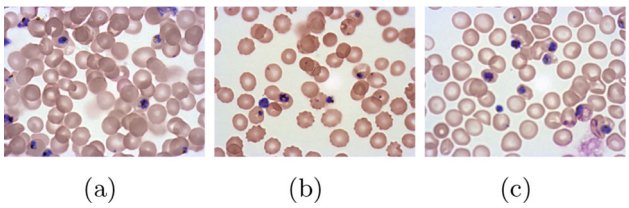

Fig. 4 Sample images from Malaria-Detection-2019: **a** ring, **b** schizont, and **c** trophozoite

4 Methodology

Our multiclass malaria classification methodology is divided into two parts. Firstly, we classify the malaria parasite type using the MP-IDB dataset. Secondly, we classify the malaria parasite life cycle stage using MP-IDB, IML_Malarai, and Malaria-Detection-2019 datasets. In this section, we explain all the preprocessing steps taken to prepare the dataset for both of the multi-class classification tasks. We also introduce the proposed architecture and other compared models used in the experiments section and the parameters chosen for training the datasets. For both malaria parasite type and life cycle stage classification we have used the same training pipeline as shown in Fig. 7. A pseudo-code of the proposed pipeline is also shown in Algorithm 1 for a better understanding of the process.

4.1 Preprocessing

All the datasets were randomly divided into training and testing sets with an 80:20 ratio. For both multi-class classification tasks, we normalize the images using mean and standard deviation. For the malaria parasite-type classification, we used the full-slide blood smear images as shown in the sample images of the previous section. Whereas, in the malaria life cycle stage classification, we cropped the IML_Malaria and Malaria-Detection-2019 datasets around the infected labeled cells using the location information provided in the annotation files of these datasets. As MP-IDB2 dataset with life cycle stage classification explained in section 3.1 was already provided in crops around the infected labeled cells. The images of all three datasets used for malaria life cycle stage classification (IML_Malaria, Malaria-Detection-2019, and MP-IDB2) become symmetrical. The sample images of crops obtained from these datasets can be seen in Fig. 5.

Due to the high imbalance of classes in most datasets, there was a high probability of the networks overfitting on the most represented classes in the training dataset. Hence several different augmentations were used to overcome this issue. The augmentations used in our study include random crop, random pad, and horizontal and vertical flips. These augmentations were applied independently for each batch

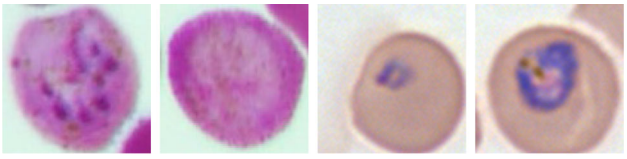

(a) (b) (c) (d)

Fig. 5 Malaria life cycle stage crops obtained from parasite location anchors, **a** schizont, **b** gametocyte, **c** ring, and d trophozoite. Here **a** and **b** are derived from IML_Malaria dataset, and **c** and **d** are derived from the Malaria-Detection-2019 dataset

with a probability of 0.5. After the augmentations, the input images (both full-slide images and crops) are resized to 224×224 for all the other architectures and 299×299 for InceptionV3. These preprocessing and augmentation steps are also defined in line 3 of our methodology Algorithm 1. The images are then converted to tensors as a standard input format. The statistical details of all the datasets used in our study, including the total number of full-slide images, crop images, and augmented images, are presented in Table 1.

4.2 Proposed architecture

We propose a less complicated yet efficient deep learning architecture for malaria-type classification and life cycle detection. The first layers of this network are the convolution layers and are translation invariant. Hence they can detect objects (cells in our case) even when the image is augmented. In our convolution layers, we have used a kernel size of 3×3 as the smaller kernels have proved to be more efficient in grasping meaningful information. We have used five convolutional layers in our network followed by MaxPool and ReLu layers. The MaxPool layers further reduce the feature map dimensions and the activation function ReLu (Rectified Linear Unit) converts all negative values to zero while keeping the positive values unchanged. Afterward, we use a global average pooling (GAP) layer. Global average pooling (Eq. 1) down-samples the feature maps to a single average value, reducing the spatial dimensionality while saving the important information.

$$\mathrm{GAP(c)} = \frac{1}{HW} \times \sum_{i=1}^{H} \sum_{j=1}^{W} F(i,j,c) \tag{1}$$

Here *GAP(c)* represents the average value of channel c, H and W stand for the height and width of the feature map, and the feature map $F(i, j, c)$ gives the value at the location of *(i,j)* in channel c.

In our case, the input of the global average pool is $256 \times 7 \times 7$ feature maps and it outputs an average of all 7 feature maps as $256 \times 1 \times 1$. This GAP layer is used to replace the fully connected layers and reduce the number of parameters. GAP layers also help in eliminating overfitting and are useful in cases where the dataset is small. Lastly, the feature maps are flattened and passed to a linear layer to be classified into the four class labels. The proposed architecture is shown pictorially in Fig. 6.

We also used several deep learning architectures and conducted numerous experiments using the pre-trained networks already available in PyTorch [37], including ResNet18 [38], Densenet121 [39], Alexnet [40], Squeezenet [41], VGG11 [42], and Inceptionv3 [43]. Details of these architectures and the proposed model are given in Table 7. It can be noted that the proposed model has the least number of trainable parameters, making it three times lighter than SqueezeNet and twenty times lighter than DenseNet. Having less than 0.4 million parameters, this network becomes the optimal lightweight network to be deployed in mobile applications and computer-aided diagnosis systems.

Algorithm 1 Algorithm for malaria classification

Require: Input image **I**, consisting of malaria slides
Ensure: Predicted class of the input image **I**
1: Convert image **I** to grayscale
2: **if** $p \geq 0.5$ **then** ▷ P is random probability
3: Apply random resize, random crop, random pad, random rotate, horizontal flip, and vertical flip to **I**
4: **end if**
5: Normalize **I** and resize to 224×224
6: Extract features by passing **I** through the hidden layers of the proposed architecture
7: Classifying **I** into four predicted classes **return** Predicted class of malaria parasite

4.3 Training

Initially, we used the architectures mentioned in the above section with two different optimizers for training over the multiclass classification of malaria parasite type, called stochastic gradient descent (SGD) and adaptive moment estimation (Adam). The Adam optimizer gave us better results so we used it in the multiclass classification of malaria life cycle stage as well. The LR of 0.001 was used with a Scheduler of step size=1. For the loss calculation, we used cross-entropy loss. It is particularly useful for unbalanced classes and works with non-normalized logits as input for each class. For both malaria parasite type and life cycle stage classification, this training and testing describes the steps in second half of our pipeline, as shown

Table 1 Statistics of the data used in malaria parasite-type and life cycle stage classification

Dataset	Full	Crops	Augmented	Classes	Resolution
MP-IDB	210	–	105	4	224†
MP-IDB2	–	1361	680	4	224†
IML_Malaria	–	427	213	4	224†
md-2019	–	1361	680	3	224†

* Here Full refers to the full-slide images used in malaria parasite-type classification and crops refers to the infected cell cropped image in the life cycle stage classification task. † Input image is resized to this resolution for each model in Table 7 other than InceptionV3

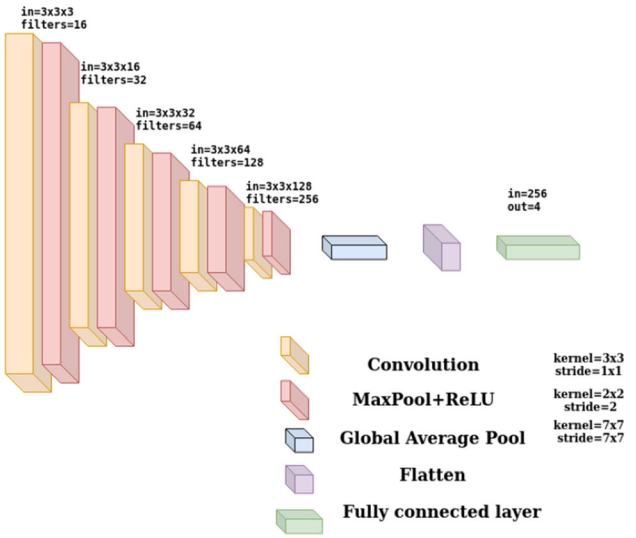

Fig. 6 Proposed malaria classification and life cycle detection architecture

in Fig. 7. However, the output label classes may vary depending on the dataset used.

All the training was done for 100 epochs and different metrics were computed to gauge the model's performance. A test can result in one of four possible outcomes: true positive (TP), false positive (FP), true negative (TN), and false negative (FN). A TP occurs when the model correctly predicts the presence of malaria parasites, aligning with the actual positive label. Conversely, an FP happens when the model incorrectly predicts the presence of parasites in an image labeled as negative. This might lead to a misdiagnosis, indicating parasites where there are none. On the other side, a TN signifies the correct identification of an absence of parasites in an image labeled as negative. Finally, an FN occurs when the model fails to detect parasites in an image labeled as positive. We use accuracy, precision, sensitivity, and F1-score to evaluate the performance of the classifiers.

Accuracy is a common metric used to evaluate the overall performance of a classification model. It is defined as the ratio of correctly predicted instances (both true positives and true negatives) to the total number of instances in the dataset.

$$\text{Accuracy} = \frac{\text{TP} + \text{FN}}{\text{TP} + \text{FP} + \text{TN} + \text{FN}} \tag{2}$$

The sensitivity is the rate of true positive, in disease detection a positive refers to the patient having that disease. So, the sensitivity (aka recall) is the model's ability to correctly diagnose an ill patient as such.

$$\text{Sensitivity} = \frac{\text{TP}}{\text{TP} + \text{FN}} \tag{3}$$

Precision measures the accuracy of the positive predictions made by the model.

$$\text{Precision} = \frac{\text{TP}}{\text{TP} + \text{FP}} \tag{4}$$

The F1-score is a valuable metric in image classification problems because it considers both false positives and false negatives, providing a balanced assessment of a model's performance, particularly in situations with imbalanced datasets.

$$\text{F1 score} = 2 \times \frac{\text{Precision} \times \text{Recall}}{\text{Precision} + \text{Recall}} \tag{5}$$

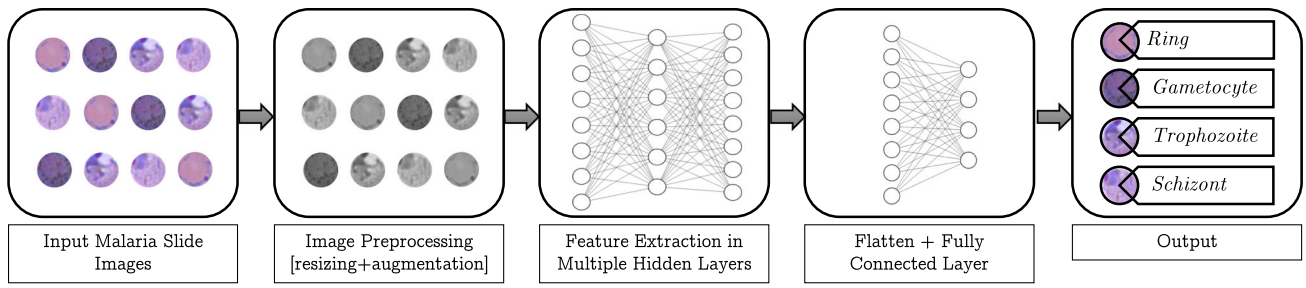

Fig. 7 Proposed malaria classification and life cycle detection pipeline

5 Results and discussion

The first part of our methodology, multiclass classification of malaria parasite type uses the MP-IDB dataset mentioned in sect. 3.1. After training for 100 epochs using the proposed architecture, we checked the classification accuracy on the test set. The multiclass classification of malaria parasite type reached an average accuracy of 99%. The individual precision, sensitivity, and F1-scores of each four classes along with the index (count frequency) of each class are shown in Table 2. The confusion matrix of each class is also represented separately in Fig. 8. It is worth noting that only one image is misclassified over the entire dataset.

The second part of our methodology corresponds to the multi-class classification of malaria life cycle stages. The proposed architecture is also trained and tested on the cell images of the MP-IDB dataset with the life cycle stage labels. The test set achieves an overall accuracy of 96% for the four mentioned life cycle stages. The indexes of all the classes, along with their individual precision sensitivity and F1-scores, are presented in Table 3. Furthermore, Fig. 9 shows the confusion matrices for this classification. These statistics show a low F1-score for the Trophozoite class. It is because this dataset is highly unbalanced as the Trophozoite and Gametocyte classes are severely underrepresented. It is also worth mentioning here that current state of the art, e.g., Loddo et al. [33] only considered the *falciparum* class, we contrastingly include all the dataset cell images instead of using only the life cycle stages of the *falciparum* class.

The second dataset we used in our multiclass classification of the malaria life cycle stage is IML_Malaria. This dataset has four balanced life cycle stages. We used the proposed network initialized from scratch for training on this dataset. Due to the balanced nature of the dataset, the individual scores of each class are better, with an overall accuracy of 92%. Table 4 refers to the individual scores of each class using all four performance parameters. The corresponding confusion matrices are shown in Fig. 10.

Table 2 Performance of the proposed algorithm on MP-IDB dataset for multiclass classification of malaria parasite type

Class	Precision	Sensitivity	F1-score	Indexes
Falciparum	1.00	1.00	1.00	6
Vivax	1.00	0.95	1.00	251
Ovale	1.00	1.00	1.00	6
Malariae	1.00	1.00	1.00	12
Average accuracy				0.99

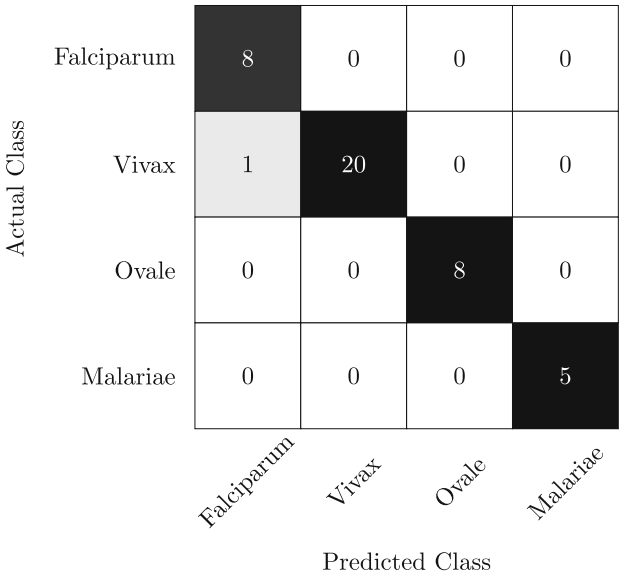

Fig. 8 Multi-class classification confusion matrix of the proposed algorithm malaria parasite-type classification on MP-IDB dataset

Table 3 Performance of the proposed model on MP-IDB2 dataset for multiclass classification of malaria life cycle stage

Class	Precision	Sensitivity	F1-score	Indexes
Gametocyte	0.80	0.67	0.73	6
Ring	0.97	1.0	0.99	251
Schizont	0.62	0.83	0.71	6
Trophozoite	1.0	0.11	0.20	12
Average accuracy				0.96

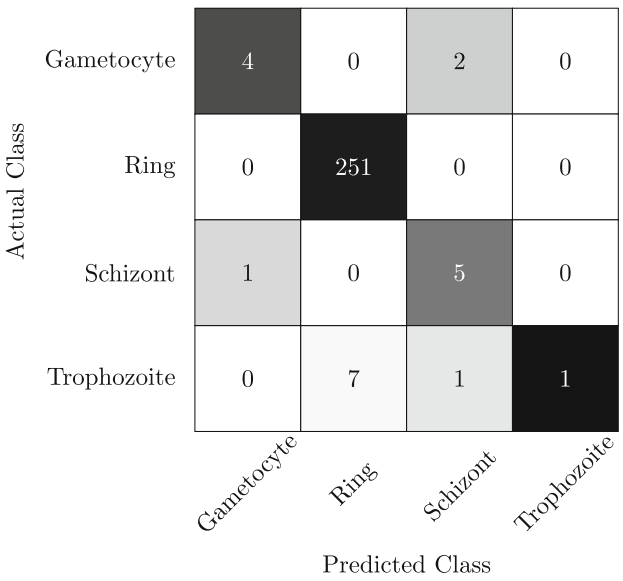

Fig. 9 Multi-class classification confusion matrix of the proposed algorithm on MP-IDB2 dataset

Table 4 Performance of the proposed model on IML_Malaria for multiclass classification of malaria life cycle stage

Class	Precision	Sensitivity	F1-score	Indexes
Gametocyte	0.91	0.98	0.95	44
Ring	0.95	0.91	0.93	22
Schizont	0.88	0.88	0.88	8
Trophozoite	0.80	0.67	0.73	12
Average accuracy				0.92

Table 5 Performance of the proposed method on Malaria-Detection-2019 for multiclass classification of malaria life cycle stage

Class	Precision	Sensitivity	F1-score	Indexes
Ring	0.83	0.87	0.85	52
Schizont	0.90	0.73	0.81	111
Trophozoite	0.73	0.87	0.79	100
Average accuracy				0.82

Lastly, we used the Malaria-Detection-2019 dataset. The given eight life stage classes are merged to make three final classes, called ring, schizont, and trophozoite. The overall accuracy achieved by our proposed network is 82%, which is comparable to Abbas et al. [34]. Although Abbas et al. [34] collected and used 112 features along with random forests to classify this dataset, the tailored collection of features is highly dependent upon the dataset and can vary when applied to other datasets. Hence our methodology is more robust and generalizable. The individual scores of each class are mentioned in Table 5, and the corresponding confusion matrices are shown in Fig. 11.

In Table 6, we provide a performance comparison between the proposed method and the state-of-the-art representative method for each dataset. On malaria-type classification problems, the proposed method achieves 99% compared to 91% of Yang [44]. On life cycle stage detection, the proposed method outperforms the Arshad [14] method by significant margins and gives comparable results to Abbas [34] without any tailored collection of features. The performance of the proposed method on MP-IDB2 is also appreciable as it achieves 96% accuracy on the entire dataset when compared to Luddo [33] which achieved 99% accuracy but only for *falciparum* class of the dataset.

All the results acquired using our novel deep learning approach beat the previous state-of-the-art results by a

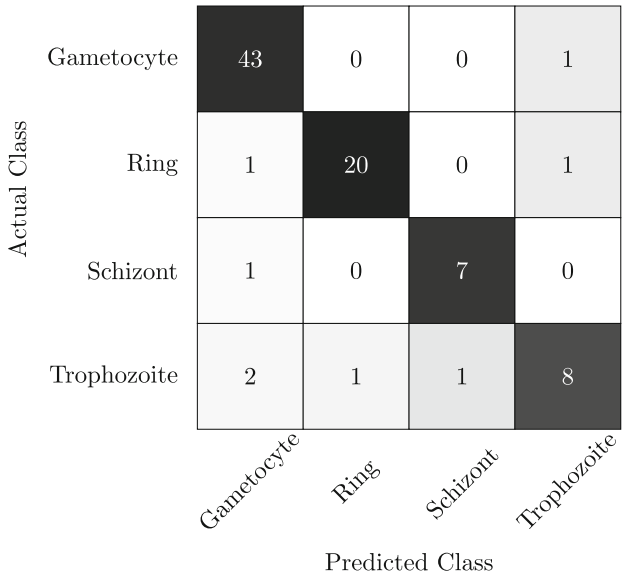

Fig. 10 Multi-class classification confusion matrix of the proposed algorithm on IML_Malaria dataset

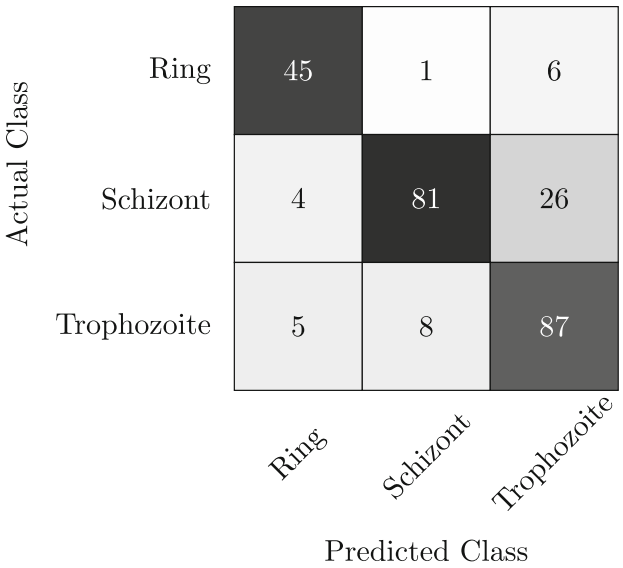

Fig. 11 Multi-class classification confusion matrix of the proposed algorithm on Malaria-Detection-2019 dataset

Table 6 Performance comparison of the proposed with the state of the art

Dataset	Classification	Results	
		Method	Ours
MP-IDB	Malaria type	Yang [44]: 91%	99%
MP-IDB2	Life cycle	Luddo [33]: 99%*	96%†
IML_Malaria	Life cycle	Arshad [14]: 80%	92%
MD-2019	Life cycle	Abbas [34]: 82%	82%

* This accuracy is only for the falciparum class of the dataset

† This accuracy is achieved for the entire dataset

Table 7 Comparison malaria-type classification accuracy of the proposed and other deep learning architectures on MP-IDB dataset

Model	Accuracy	Flops	Inference batch=1	Parameters
ResNet18	0.98	1.82G	0.43s	11,178,564
DenseNet121	0.95	2.88G	0.28s	7,978,856
SqueezeNet	0.86	743.36M	0.08s	1,248,424
AlexNet	0.93	711.47M	0.95s	57,020,228
VGG11	0.98	7.64G	1.70s	128,788,228
InceptionV3	0.90	5.73G	0.49s	24,354,536
Proposed	0.99	256.01M	0.03s	393,636

* The input image size of 224 × 224 is used for all models other than Inception V3, and an input size of 299 × 299 is used for Inception V3

clear margin. The convolution layers in our network focus on the vital information present in the input images and the GAP layer averages this information while preserving the spatial dimension. Due to the combination of these layers, our network is able to provide better results in a cost-efficient manner while avoiding overfitting. The state-of-the-art deep learning architectures rely on large datasets to learn better and give optimal results. In this problem, as the datasets are small, these deep learning architectures overfit and gave better results than our architecture on the training set images but worse on the test set. The comparison between the previous state of the art and our results is presented in Table 7. Our proposed architecture gives better accuracy results than ResNet (the closest competitor) on MP-IDB dataset, with six times lower Flops (floating point operations per second) and 13% faster inference time proving that our architecture is more cost and time-efficient.

Furthermore, as these datasets are highly unbalanced the state-of-the-art architectures only gave good results for the most represented classes, i.e., *falciparum* and *vivax* in the malaria parasite type, and ring in the malaria life cycle stage. On the other hand, as seen in the confusion matrices, our proposed architecture emphasizes the under-represented classes and gives better precision and sensitivity values for them as compared to the other architectures. This trait makes our architecture the most suitable candidate for the unbalanced healthcare and medical datasets.

5.1 Ablation study

The main motive of this research is to propose a lightweight deep learning model that gives optimal results for the multiclass classification of malaria. To this end, we trained the proposed method on two different input resolutions, 224 × 224 and 112 × 112. The number of parameters for both input resolutions is the same, i.e., 393K, but the main measure of difference is floating point operations per second (FLOPS). FLOPS play an integral part in measuring the complexity of a deep learning model, as a higher number of FLOPS leads to more training time and slower inference speed. To save computational resources while maintaining a high accuracy score is an active research field in deep learning. In our experiments, we observed that the lower-resolution input image decreases the FLOPS considerably and is computationally more cost-effective. We present the results of this ablation in Table 8.

The image input resolution of 224 × 224 achieved the highest accuracy scores for all datasets. However, by reducing this input resolution to 112 × 112, the FLOPS decrease by four times. This reduction in computational complexity is achieved by trading off only 2 to 3% average accuracy.

6 Conclusion

In this paper, we have presented a lightweight technique for multiclass classification of malaria parasite type and life cycle stage. Our proposed architecture achieves better results than the state of the art on four benchmark malaria datasets. It also focuses on the classes with low counts, making it an ideal choice for unbalanced datasets. Moreover, our architecture is light enough to be embedded in mobile applications which will be very beneficial for the understaffed hospitals of the developing countries that lack advanced computer tools to support heavy deep learning models. To the best of our knowledge, this is the most vast and diverse study conducted for both multiclass malaria

Table 8 Impact of input resolution on the computational complexity in terms of FLOPS (floating point operations per second), and accuracy. Note: K and M denote 10^3 and 10^6, respectively

	Input Size: 224 × 224			Input Size: 112 × 112		
Dataset	Accuracy	#Params	FLOPS	Accuracy	#Params	FLOPS
MP-IDB	0.99	393K	256 M	0.93	393K	60 M
MP-IDB2	0.96	393K	256 M	0.95	393K	60 M
IML_Malaria	0.92	393K	256 M	0.91	393K	60 M
Malaria-Detection 2019	0.82	393K	256 M	0.81	393K	60 M

parasite type and life cycle stage classification on different datasets using a novel cost-efficient model. However, it can be observed from the results that the proposed life cycle classification approach struggles to achieve the desired accuracy in the Schizont and Trophozoite stages. From the initial investigations, we observed that the reasons for this limiting performance are the limited or biased dataset which results in restricted learning of the model. Furthermore, these two types appear visually similar, particularly under low-resolution imaging systems and the model fails to distinguish them. We believe that this limitation can be overcome if a sufficient dataset for training is available. In future, we would like to add more balanced datasets to our experiments to eliminate any accidental bias and embed our architecture in mobile applications and CAD systems.

Funding Open access funding provided by Università degli Studi di Torino within the CRUI-CARE Agreement.

Data availability All the data used in our study are publicly available and referenced in their relevant sections.

Declarations

Conflict of interest No conflict of interest or funding to declare.

References

1. World Health Organization (2022) World malaria report 2022. World Health Organization
2. World Health Organization (2022) Malaria - Pakistan. https://www.who.int/emergencies/disease-outbreak-news/item/2022-DON413, [Online; accessed 07-July-2023]
3. Wafula ST, Habermann T, Franke MA et al (2023) What are the pathways between poverty and malaria in sub-saharan africa? A systematic review of mediation studies. Infect Dis Poverty 12(03):13–30. https://doi.org/10.1186/s40249-023-01110-2
4. Price RN, Commons RJ, Battle KE et al (2020) Plasmodium vivax in the era of the shrinking P. falciparum map. Trends Parasitol 36(6):560–570. https://doi.org/10.1016/j.pt.2020.03.009
5. Neveu G, Lavazec C (2021) Erythroid cells and malaria parasites: it's a match! Curr Opin Hematol 28(3):158–63
6. Bousema T, Drakeley C (2011) Epidemiology and infectivity of plasmodium falciparum and plasmodium vivax gametocytes in relation to malaria control and elimination. Clin Microbiol Rev 24(2):377–410. https://doi.org/10.1128/cmr.00051-10
7. Adegoke JA, Raper H, Gassner C et al (2022) Visible microspectrophotometry coupled with machine learning to discriminate the erythrocytic life cycle stages of P. falciparum malaria parasites in functional single cells. Analyst 147:2662–2670. https://doi.org/10.1039/D2AN00274D
8. Kochan K, Bedolla DE, Perez-Guaita D et al (2021) Infrared spectroscopy of blood. Appl Spectrosc 75(6):611–646
9. White NJ (2022) Severe malaria. Malar J 21(1):284. https://doi.org/10.1186/s12936-022-04301-8
10. Mohammed HA, Abdelrahman IAM (2017) Detection and classification of malaria in thin blood slide images. In: 2017 international conference on communication, control, computing and electronics engineering (ICCCCEE), IEEE, pp 1–5, https://doi.org/10.1109/ICCCCEE.2017.7866700
11. Komagal E, Kumar K, Vigneswaran A (2013) Recognition and classification of malaria plasmodium diagnosis. Int J Eng Res Technol 2(1):1–4
12. Punitha S, Logeshwari P, Sivaranjani P et al (2017) Detection of malarial parasite in blood using image processing. Asian J Appl Sci Technol 1(2):211–213
13. Razzak MI (2015) Automatic detection and classification of malarial parasite. Int J Biom Bioinform (IJBB) 9(1):1–12
14. Arshad QA, Ali M, Hassan SU et al (2021) A dataset and benchmark for malaria life-cycle classification in thin blood smear images. Neural Comput Appl 34(6):4473–4485. https://doi.org/10.1007/s00521-021-06602-6
15. Liang Z, Powell A, Ersoy I, et al (2016) Cnn-based image analysis for malaria diagnosis. In: 2016 IEEE international conference on bioinformatics and biomedicine (BIBM), IEEE, pp 493–496
16. Pan WD, Dong Y, Wu D (2018) Classification of malaria-infected cells using deep convolutional neural networks, vol 159, IntechOpen
17. Fatima T, Farid MS (2019) Automatic detection of plasmodium parasites from microscopic blood images. J Parasit Dis 44(1):69–78. https://doi.org/10.1007/s12639-019-01163-x
18. Rahman A, Zunair H, Rahman MS, et al (2019) Improving malaria parasite detection from red blood cell using deep convolutional neural networks. arXiv preprint arXiv:1907.10418arXiv:1907.10418 [eess.IV]
19. Rajaraman S, Antani SK, Poostchi M et al (2018) Pre-trained convolutional neural networks as feature extractors toward improved malaria parasite detection in thin blood smear images. PeerJ 6:e4568
20. Quinn JA, Nakasi R, Mugagga PKB, et al (2016) Deep convolutional neural networks for microscopy-based point of care diagnostics. In: Doshi-Velez F, Fackler J, Kale D, et al (eds) Proceedings of the 1st Machine Learning for Healthcare Conference, Proceedings of Machine Learning Research, vol 56. PMLR, Northeastern University, Boston, MA, USA, pp 271–281, https://proceedings.mlr.press/v56/Quinn16.html
21. Savkare S, Narote S (2015) Automated system for malaria parasite identification. In: 2015 international conference on communication, information & computing technology (ICCICT), IEEE, pp 1–4
22. Fn KT, Daniel T, Pierre E et al (2016) Automated diagnosis of malaria in tropical areas using 40x microscopic images of blood smears. Int J Biom Bioinforma 10(2):12
23. Kareem S, Kale I, Morling RC (2012) Automated malaria parasite detection in thin blood films:-a hybrid illumination and color constancy insensitive, morphological approach. In: 2012 IEEE Asia Pacific Conference on Circuits and Systems, IEEE, pp 240–243, https://doi.org/10.1109/APCCAS.2012.6419016

24. May Z, Mohd Aziz SSA, Salamat R (2013) Automated quantification and classification of malaria parasites in thin blood smears. In: 2013 IEEE International Conference on Signal and Image Processing Applications, pp 369–373, https://doi.org/10.1109/ICSIPA.2013.6708035
25. Roy K, Sharmin S, Mukta RM et al (2018) Detection of malaria parasite in giemsa blood sample using image processing. Int J Comput Sci Inform Technol 10(1):55–65
26. Arco J, Górriz J, Ramírez J et al (2015) Digital image analysis for automatic enumeration of malaria parasites using morphological operations. Expert Syst Appl 42(6):3041–3047
27. Umer M, Sadiq S, Ahmad M et al (2020) A novel stacked cnn for malarial parasite detection in thin blood smear images. IEEE Access 8:93782–93792. https://doi.org/10.1109/ACCESS.2020.2994810
28. Gautam K, Jangir SK, Kumar M, et al (2020) Malaria detection system using convolutional neural network algorithm. In: Machine learning and deep learning in real-time applications. IGI Global, p 219–230. https://doi.org/10.4018/978-1-7998-3095-5.ch010
29. Maqsood A, Farid MS, Khan MH et al (2021) Deep malaria parasite detection in thin blood smear microscopic images. Appl Sci 11(5):2284. https://doi.org/10.3390/app11052284
30. Imran T, Khan MA, Sharif M et al (2022) Malaria blood smear classification using deep learning and best features selection. Computers, Materials Continua. 70(1):1875–1891. https://doi.org/10.32604/cmc.2022.018946
31. Loddo A, Di Ruberto C, Kocher M, et al (2019) MP-IDB: the malaria parasite image database for image processing and analysis. In: Processing and Analysis of Biomedical Information: First International SIPAIM Workshop, SaMBa 2018, Held in Conjunction with MICCAI 2018, Granada, Spain, September 20, 2018, Revised Selected Papers 1, Springer, pp 57–65
32. Kassim YM, Yang F, Yu H et al (2021) Diagnosing malaria patients with plasmodium falciparum and vivax using deep learning for thick smear images. Diagnostics 11(11):1994. https://doi.org/10.3390/diagnostics11111994
33. Loddo A, Fadda C, Di Ruberto C (2022) An empirical evaluation of convolutional networks for malaria diagnosis. J Imaging 8(3):66
34. Abbas SS, Dijkstra TMH (2020) Detection and stage classification of plasmodium falciparum from images of giemsa stained thin blood films using random forest classifiers. Diagn Pathol 15(1):130. https://doi.org/10.1186/s13000-020-01040-9
35. Azhar MS, Mashor MY, Kanafiah A, et al (2023) Development of life cycle classification system for plasmodium knowlesi malaria species using deep learning. In: AIP Conference Proceedings, AIP Publishing
36. Araujo F, Colares N, Carvalho U, et al (2023) Plasmodium life cycle-stage classification on thick blood smear microscopy images using deep learning: A contribution to malaria diagnosis. In: 2023 19th International Symposium on Medical Information Processing and Analysis (SIPAIM), IEEE, pp 1–4
37. Paszke A, Gross S, Massa F, et al (2019) Pytorch: An imperative style, high-performance deep learning library. In: Wallach H, Larochelle H, Beygelzimer A, et al (eds) Advances in Neural Information Processing Systems, vol 32. Curran Associates, Inc., https://proceedings.neurips.cc/paper_files/paper/2019/file/bdbca288fee7f92f2bfa9f7012727740-Paper.pdf
38. He K, Zhang X, Ren S, et al (2016) Deep residual learning for image recognition. In: Proceedings of the IEEE conference on computer vision and pattern recognition. (CVPR), pp 770–778, https://doi.org/10.1109/CVPR.2016.90
39. Huang G, Liu Z, Maaten LVD, et al (2017) Densely connected convolutional networks. In: Proceedings of the IEEE conference on computer vision and pattern recognition. (CVPR). IEEE Computer Society, Los Alamitos, CA, USA, pp 2261–2269, https://doi.org/10.1109/CVPR.2017.243,
40. Krizhevsky A, Sutskever I, Hinton GE (2017) Imagenet classification with deep convolutional neural networks. Commun ACM 60(6):84–90. https://doi.org/10.1145/3065386
41. Iandola FN, Han S, Moskewicz MW, et al (2016) Squeezenet: Alexnet-level accuracy with 50x fewer parameters and<1mb model size. arXiv preprint arXiv:1602.07360
42. Simonyan K, Zisserman A (2014) Very deep convolutional networks for large-scale image recognition. arXiv preprint arXiv:1409.1556
43. Szegedy C, Vanhoucke V, Ioffe S, et al (2016) Rethinking the inception architecture for computer vision. In: Proc. IEEE Conf. Comput. Vis. Pattern Recognit. (CVPR), pp 2818–2826, https://doi.org/10.1109/CVPR.2016.308
44. Yang Z, Benhabiles H, Hammoudi K et al (2022) A generalized deep learning-based framework for assistance to the human malaria diagnosis from microscopic images. Neural Comput Appl 34(17):14223–14238. https://doi.org/10.1007/s00521-021-06604-4